JAERI-M
87-119

TWO-DIMENSIONAL ANALYSIS FOR A SCRAPEOFF AND DIVERTOR REGIONS WITH AN MHD MODEL

—CONCEPTUAL DESIGN STUDY OF FY86 FER—

August 1987

Noriaki UEDA[*1], Masao KASAI[*1], Shigehisa HITOKI[*2], Noboru FUJISAWA
Masayoshi SUGIHARA, Shin YAMAMOTO, Tadanori MIZOGUCHI,[*3]
Mitsushi ABE,[*4] Takashi OKAZAKI,[*4] Kunihiko OKANO[*5], Kichiro SHINYA[*5]
and Akiyoshi HATAYAMA[*3]

日本原子力研究所
Japan Atomic Energy Research Institute

JAERI-Mレポートは，日本原子力研究所が不定期に公刊している研究報告書です。
入手の問合わせは，日本原子力研究所技術情報部情報資料課（〒319-11茨城県那珂郡東海村）あて，お申しこしください。なお，このほかに財団法人原子力弘済会資料センター（〒319-11 茨城県那珂郡東海村日本原子力研究所内）で複写による実費頒布をおこなっております。

JAERI-M reports are issued irregularly.
Inquiries about availability of the reports should be addressed to Information Division Department of Technical Information, Japan Atomic Energy Research Institute, Tokai-mura, Naka-gun, Ibaraki-ken 319-11, Japan.

編集兼発行　日本原子力研究所
印　　刷　いばらき印刷㈱

JAERI-M 87-119

Two-Dimensional Analysis for a Scrapeoff and Divertor Regions with an MHD Model — Conceptual Design Study of FY86 FER —

Noriaki UEDA*1, Masao KASAI*1, Shigehisa HITOKI*2
Noboru FUJISAWA, Mosayoshi SUGIHARA, Shin YAMAMOTO
Tadanori MIZOGUCHI*3, Mitsushi ABE*4, Takashi OKAZAKI*4
Kunihiko OKANO*5, Kichiro SHINYA*5 and Akiyoshi HATAYAMA*5

Department of Large Tokamak Research
Naka Fusion Research Establishment
Japan Atomic Energy Research Institute
Naka-machi, Naka-gun, Ibaraki-ken

(Received July 21, 1987)

With a two-dimensional time dependent fluid code for transport processes in the edge plasma in a tokamak, coupled with Monte-Carlo method for neutral gas behavior, preliminary numerical study has been carried out for the FER divertor. Design base data such as energy flux, particle flux and so on which are essentially important to make an divertor design reliable have been obtained.

Keywords : Scrapeoff Layer, Divertor, MHD Equation, Neutral Gas, Simulation, Particle in Cell Method

---

*1 Mitsubishi Atomic Power Industries, Inc.
*2 On leave from Mitsubishi Electric Co.
*3 On leave from Hitachi Ltd.
*4 Hitachi Ltd.
*5 Toshiba Corporation

JAERI－M 87－119

2次元流体コードによるスクレイプオフ及びダイバータ領域のプラズマ挙動解析
--次期大型装置設計（FY86FER）－

日本原子力研究所那珂研究所臨界プラズマ研究部
上田憲照[*1]・笠井雅夫[*1]・一木繁久[*2]・藤沢　登　・杉原正芳
山本　新　・溝口忠憲[*3]・阿部充志[*4]・岡崎隆司[*4]・岡野邦彦[*5]
新谷吉郎[*5]・畑山明聖[*5]

（1987年7月21日受理）

エッジプラズマの挙動を2次元流体モデルで表現し，更に中性粒子挙動についてはMonte－Carlo 法で解くコードを用い，FERのダイバータの予備解析を実施した結果エネルギや粒子フラックス等の設計に不可欠の基本データを得た。

那珂研究所：〒311－02 茨城県那珂郡那珂町大字向山801－1
＊1　三菱原子力工業
＊2　外来研究員三菱電機（株）
＊3　外来　〃　（株）日立製作所
＊4　（株）日立製作所
＊5　（株）東芝

Contents

目　　次

1. Introduction

The impurity and particle control is one of the critical issues to realize the next generation fusion reactor such as FER, NET, INTOR and other large machines [1]. Poloidal divertor has been chosen as the major candidate for an impurity and particle control system and many efforts have been made until now both in experiments and numerical approach to clarify the divertor behavior.

For modeling of a divertor, there are at least two codes which deal with the behavior of the scrapeoff and divertor plasma in a two-dimensional space. They are the PLANET code [2] at PPPL and Braams code [3]. The former code uses Monte-Carlo method to calculate neutral behavior. Both codes can give a realistic modeling of the scrapeoff and divertor plasma to some extent. The shortcoming of the codes is that some artificial boundary conditions must be given at the boundary of the domain of calculation. In other words, it can not treat the free boundary of the diffusing plasma.

In the actual design of divertor or limiter, it is important to calculate the radial diffusion process for accurate estimation of particle and energy deposition on the structures. It is also important to estimate coupling efficiency of the RF launcher. For this, it is required to be able to treat the free boundary problem.

To coup with these problems, a two-dimensional time dependent fluid code has been developed. The code employs the Particle In Cell (PIC) method [4] for numerical solution of Braginskii transport equation. Also, neutral particle calculation package by Monte-Carlo method is available with this code.

A code verification or comparison between the predictions with this code and existing divertor experiments has been successfully performed [5].

This time, using the code, preliminary analyses of divertor and scrapeoff plasma of the FER has been carried out. In the simulation of reactor size plasma, it may be important to take into account the behavior of impurity ion and neutrals. In this code, Neuhauser's impurity model has been used for Helium ions.

Another important tasks to be solved in this field are,

(1) compatibility between cold and dense divertor and H mode,

(2) ash exhaust and particle control,

(3) recycling rate and redeposition,

and so on. We will refer to these problems in the near future.

2. Modeling of the boundary plasma

2.1 The geometry of the scrapeoff and divertor region

The poloidal cross-section of the D-III for example with the domain of the calculation is shown in Fig. 1. There are three regions to be considered; core plasma, scrapeoff and diverted plasma and vacuum regions. In this code, transport of the core plasma is not solved, so, the prescribed particle flux Γ and energy fluxes Q_e and Q_i for electron and ion are respectively to be given at the boundary of the core plasma.

In the scrapeoff and diverted plasma region, the fluid equation and neutral gas transport are to be solved. The orthogonal coordinate ψ and z which correspond to the poloidal flux and the poloidal length of the magnetic line of force are respectively employed for the fluid equations. The region is divided into small cells (i,j), where i and j denote the cell number in the z (from i=4 to 44 in this case) and ψ (from j=1 to 9) coordinates.

In the vacuum region, only neutral gas transport is solved. The behavior of the neutral gas is calculated with Monte-Carlo method. The neutral gas calculation package is called every several tenth of the fluid calculation time cycle to save computation time.

2.2 Fluid equations

A set of equations for the scrapeoff and divertor plasma is made up of a continuity equation for the ion density, a momentum conservation equation governing the parallel velocity $v_{//}$, a diffusion equation for the perpendicular velocity v_ψ and energy conservation equations for the electron and ion temperatures T_e and T_i. Using the continuity equation for the ion density, the momentum and energy conservation equations are written as follows

(3) recycling rate and redeposition,

and so on. We will refer to these problems in the near future.

2. Modeling of the boundary plasma

2.1 The geometry of the scrapeoff and divertor region

The poloidal cross-section of the D-III for example with the domain of the calculation is shown in Fig. 1. There are three regions to be considered; core plasma, scrapeoff and diverted plasma and vacuum regions. In this code, transport of the core plasma is not solved, so, the prescribed particle flux Γ and energy fluxes Q_e and Q_i for electron and ion are respectively to be given at the boundary of the core plasma.

In the scrapeoff and diverted plasma region, the fluid equation and neutral gas transport are to be solved. The orthogonal coordinate ψ and z which correspond to the poloidal flux and the poloidal length of the magnetic line of force are respectively employed for the fluid equations. The region is divided into small cells (i,j), where i and j denote the cell number in the z (from i=4 to 44 in this case) and ψ (from j=1 to 9) coordinates.

In the vacuum region, only neutral gas transport is solved. The behavior of the neutral gas is calculated with Monte-Carlo method. The neutral gas calculation package is called every several tenth of the fluid calculation time cycle to save computation time.

2.2 Fluid equations

A set of equations for the scrapeoff and divertor plasma is made up of a continuity equation for the ion density, a momentum conservation equation governing the parallel velocity $v_{//}$, a diffusion equation for the perpendicular velocity v_ψ and energy conservation equations for the electron and ion temperatures T_e and T_i. Using the continuity equation for the ion density, the momentum and energy conservation equations are written as follows

$$\rho_i \left(\frac{\partial}{\partial t} + \vec{v}\cdot\nabla\right)\vec{v}_{//} = - \frac{B_\theta}{B_T} \frac{1}{h_z} \frac{\partial P}{\partial z} - S_n \vec{v}_{//} \ , \tag{1}$$

$$\vec{v}_\psi = - \frac{1}{h_\psi} \frac{D}{n_i} \frac{\partial n_i}{\partial \psi} \ , \tag{2}$$

$$\rho_i \left(\frac{\partial}{\partial t} + \vec{v}\cdot\nabla\right) \left(\frac{3}{2} \frac{kT_i}{m_i} + \frac{1}{2} \vec{v}\cdot\vec{v}\right)$$

$$= -\nabla\cdot\left(\frac{\rho_i kT_i}{m_i} \vec{v}\right) - \vec{v}\cdot\nabla \left(\frac{\rho_e kT_e}{m_e}\right) + \nabla\cdot\kappa_i\nabla \left(kT_i\right) - E_s^i S_n^i + Q_{ei} - Q_{cx} \ , \tag{3}$$

$$\rho_e \left(\frac{\partial}{\partial t} + \vec{v}\cdot\nabla\right) \left(\frac{3}{2} \frac{kT_e}{m_e} + \frac{1}{2} \vec{v}\cdot\vec{v}\right)$$

$$= -\nabla\cdot\left(\frac{\rho_e kT_e}{m_e} \vec{v}\right) + \vec{v}\cdot\nabla \left(\frac{\rho_e kT_e}{m_e}\right) + \nabla\cdot\kappa_e\nabla \left(kT_e\right) - E_s^e S_n^e - Q_{ei} - Q_{rad} \ , \tag{4}$$

where S_n is the volume source of ions. Q_{ei} is the electron-ion energy equilibration term. Q_{rad} is the radiation loss. D is the radial anomalous diffusion coefficient. h_z and h_ψ are metric coefficients. Auxiliary relations are $n_e=n_i\cdot Z_i$ where Z_i is the ion charge number, the total and partial pressures, $P_T=P_e+P_i$ and total energy E_s,

$$E_s^{i,e} = \rho_{i,e} \left(I_{i,e} + \frac{1}{2} \vec{v}\cdot\vec{v}\right) \ .$$

In the above equation, I is the specific internal energy ($I = \frac{3kT}{2m}$). The poloidal flow velocity v_z is calculated as

$$v_z = v_{//}(B_\theta/B_T) \ , \tag{5}$$

where B_θ and B_T are poloidal and toroidal field respectively. Also, the poloidal heat conduction coefficient κ_z is related to classical parallel coefficient according to

$$\kappa_z = \kappa_{//}(B_\theta/B_T)^2 \ . \tag{6}$$

2.3 Numerical method

Numerical method adopted to solve the fluid equations in this code is the PIC method. The PIC employs both an Eulerian and a Lagrangian mesh. The resion, through which the fluid moves, is subdivided into a finite mesh of Eulerian cells which are fixed relative to the observer. Associated with the center of each cell are a velocity, an internal energy, and the total mass of each kind of material. The calculation develops the history of each of these variables with time. In addition, the fluid itself is represented by Lagrangian mass points, or particles, which move through the Eulerian mesh, thus representing the motion of the fluid.

calculation procedures consist of three steps according to the PIC scheme. In the first step, the Lagrangian method is employed. So, dropping the transport term in Eq. (1), we calculate the tentative velocity $\tilde{v}_{\shortparallel}$ by the following equation,

$$\rho_i \frac{\tilde{v}_{\shortparallel} - v_{\shortparallel}^n}{\Delta t} = - \frac{B_\theta}{B_T} \frac{1}{h_z} \frac{\partial P}{\partial z} , \tag{7}$$

where "~" denotes tentative value owing to neglect of the material transport, which will be rectified later. $v_{\shortparallel}^n$ is the parallel velocity at former step (n-th time step). In this equation, the second term on the right hand side in Eq. (1) is also dropped at this step because it is related to particle annihilation and generation. P has been determined by the equation of state at the former step. The tentative temperature $\tilde{T}$ or internal energy $\tilde{I}$ is calculated by the following equations in the same manner as mentioned above,

$$\rho_e \left[\frac{3}{2} \frac{k}{m_e} (\tilde{T}_e - T_e^n) + \frac{1}{2} \{(\tilde{\vec{v}})^2 - (\vec{v}^n)^2\}\right]/\Delta t$$

$$= -\nabla\cdot\left(\frac{\rho_e k\tilde{T}_e}{m_e} \tilde{\vec{v}}\right) + \tilde{\vec{v}}\cdot\nabla \left(\frac{\rho_e k\tilde{T}_e}{m_e}\right) + \nabla\cdot\kappa_e\nabla (k\tilde{T}_e) - Q_{ei} - Q_{rad} , \tag{8}$$

$$\rho_i \left[\frac{3}{2} \frac{k}{m_i} (\tilde{T}_i^n) + \frac{1}{2} \{(\tilde{\vec{v}})^2 - (\vec{v}^n)^2\}\right]/\Delta t$$

$$= -\nabla\cdot\left(\frac{\rho_i k\tilde{T}_i}{m_i} \tilde{\vec{v}}\right) - \tilde{\vec{v}}\cdot\nabla \left(\frac{\rho_e k\tilde{T}_e}{m_e}\right) + \nabla\cdot\kappa_i\nabla (k\tilde{T}_i) - Q_{ei} - Q_{cx} , \tag{9}$$

2.3 Numerical method

Numerical method adopted to solve the fluid equations in this code is the PIC method. The PIC employs both an Eulerian and a Lagrangian mesh. The resion, through which the fluid moves, is subdivided into a finite mesh of Eulerian cells which are fixed relative to the observer. Associated with the center of each cell are a velocity, an internal energy, and the total mass of each kind of material. The calculation develops the history of each of these variables with time. In addition, the fluid itself is represented by Lagrangian mass points, or particles, which move through the Eulerian mesh, thus representing the motion of the fluid.

calculation procedures consist of three steps according to the PIC scheme. In the first step, the Lagrangian method is employed. So, dropping the transport term in Eq. (1), we calculate the tentative velocity $\tilde{v}_{\shortparallel}$ by the following equation,

$$\rho_i \frac{\tilde{v}_{\shortparallel} - v_{\shortparallel}^n}{\Delta t} = - \frac{B_\theta}{B_T} \frac{1}{h_z} \frac{\partial P}{\partial z} , \tag{7}$$

where "~" denotes tentative value owing to neglect of the material transport, which will be rectified later. $v_{\shortparallel}^n$ is the parallel velocity at former step (n-th time step). In this equation, the second term on the right hand side in Eq. (1) is also dropped at this step because it is related to particle annihilation and generation. P has been determined by the equation of state at the former step. The tentative temperature $\tilde{T}$ or internal energy $\tilde{I}$ is calculated by the following equations in the same manner as mentioned above,

$$\rho_e \left[\frac{3}{2} \frac{k}{m_e} (\tilde{T}_e - T_e^n) + \frac{1}{2} \{(\tilde{\vec{v}})^2 - (\vec{v}^n)^2\}\right]/\Delta t$$

$$= -\nabla\cdot\left(\frac{\rho_e k \tilde{T}_e}{m_e} \tilde{\vec{v}}\right) + \tilde{\vec{v}}\cdot\nabla \left(\frac{\rho_e k \tilde{T}_e}{m_e}\right) + \nabla\cdot\kappa_e\nabla (k\tilde{T}_e) - Q_{ei} - Q_{rad} , \tag{8}$$

$$\rho_i \left[\frac{3}{2} \frac{k}{m_i} (\tilde{T}_i^n) + \frac{1}{2} \{(\tilde{\vec{v}})^2 - (\vec{v}^n)^2\}\right]/\Delta t$$

$$= -\nabla\cdot\left(\frac{\rho_i k \tilde{T}_i}{m_i} \tilde{\vec{v}}\right) - \tilde{\vec{v}}\cdot\nabla \left(\frac{\rho_e k \tilde{T}_e}{m_e}\right) + \nabla\cdot\kappa_i\nabla (k\tilde{T}_i) - Q_{ei} - Q_{cx} , \tag{9}$$

where T_e^n and T_i^n are temperatures at the former step.
Since $\kappa_{//}$ has a strong temperature dependence, the coupled equations (8) and (9) are solved by the implicit method.

In the next step, we move the particle in the cell:

$$\begin{pmatrix} z^{n+1} \\ \psi^{n+1} \end{pmatrix} = \begin{pmatrix} z^n \\ \psi^n \end{pmatrix} + \begin{pmatrix} \tilde{v}_z/h_z \\ \tilde{v}_\psi/h_\psi \end{pmatrix} \Delta t \tag{10}$$

In the last calculation step, we rezone the cells (and mass points) to reintroduce the original mesh distribution. In the process, we repartition the momentum and energy as follows to obtain new spatial distribution functions without affecting the conservation of these quantities,

$$M^{n+1} = M^n - \sum_{out} m + \sum_{in} m_N + S_n v_c \Delta t \ , \tag{11}$$

$$\vec{v}^{n+1} = [(M^n - \sum_{out} m + S_n v_c \Delta t)\tilde{\vec{v}} + \sum_N (\tilde{\vec{v}}_N \sum_{in} m_N)]/M^{n+1} \ , \tag{12}$$

$$I^{n+1} = [(M^n - \sum_{out} m + S_n v_c \Delta t)\tilde{I} + \sum_N (\tilde{I}_N \sum_{in} m_N) \ ,$$

$$+ \frac{1}{2}\{(M^n - \sum_{out} m + S_n v_c \Delta t)\tilde{\vec{v}}^2 + \sum_N (\tilde{\vec{v}}^2 \sum_{in} m_N)\}]/M^{n+1} \ . \tag{13}$$

The second term in Eq. (11) denotes the sum of massess of the particles which have left the cell (i,j). The third term represents the sum of particles which have entered the cell (i,j) from the neighboring cells. The last term, $S_v v_c \Delta t$ means the gain of ions in the cell with atomic process within the time interval Δt. Summation in the second term in Eq. (12) is over those neighboring cells from which particles have entered the cell (i,j).

2.4 Boundary conditions of the fluid equations

In the computational mesh shown in Fig. 1, there are three boundaries for the fluid equations: surface of the divertor plate, surface of the vacuum vessel and periphery of the core plasma. At the divertor plate, following sheath criterion is employed for the parallel fluid velocity,

$$v_{//} = \sqrt{(T_e + T_i)/\rho_i} \ .$$

Also, at the divertor plate, $\nabla_{//}T_e$ and $\nabla_{//}T_i$ are specified as follows,

$$- \kappa^e_{//}\nabla_{//}T_e = \gamma n_e \vec{v}_{//}T_e \ ,$$

$$\nabla_{//}T_i = 0 \ ,$$

where γ is equal to 1.8 when no secondary electron emission is considered.

At the surface of the vacuum vessel, gradients of the pressure and temperature are set to zero in this code.

Along the boundary of the core plasma, a prescribed input of particle and energy fluxes to the scrapeoff layer is inserted. The radial flow velocity of the particles at the boundary v^B_ψ is determined by the diffusion equation Eq. (1) as follows,

$$v^B_\psi = \Gamma/(\rho_c - \frac{\Gamma}{D}\frac{h_\psi \delta\psi}{2}) \ ,$$

where Γ is the prescribed particle flux from the core plasma. $\delta\psi$ is the increment of ψ. ρ_c is the density of the cell located in the scrapeoff layer adjacent to the boundary of the core plasma. The energy fluxes Q_e and Q_i across the boundary consist of the following terms,

$$Q_e = - \kappa^e_\psi \nabla_\psi (kT_e) + \frac{k}{m_e}\Gamma_e T^B_e - v_c \frac{k}{m_e}\rho^B_e T^B_e + \frac{3}{2}\frac{k}{m_e}\Gamma_e T^B_e + \frac{1}{2}\rho^B_e v^{B2}_\psi \ ,$$

$$Q_i = - \kappa^i_\psi \nabla_\psi (kT_i) + \frac{k}{m_i}\Gamma_i T^B_i + v_c \frac{k}{m_e}\rho^B_e T^B_e + \frac{3}{2}\frac{k}{m_i}\Gamma_i T^B_i + \frac{1}{2}\rho^B_i v^{B2}_\psi \ ,$$

where v_c denotes the velocity of the cell located in the scrapeoff layer adjacent to the boundary of the core plasma. In the equations, T^B_e and T^B_i are determined by the difference forms of these simultaneous equations. In this code, the first three terms on the right hand side of these equations are taken into account in the first step of the PIC calculational step mentioned before. The sum of the remaining two terms, which means the total energy carried with particle movement, is taken into account in the third step.

3. Numerical simulation of the FER divertor plasma

In the simulation of reactor size plasma, it is important to include the behavior of impurities which arise from the sputtering, vaporization of the structural material by heat concentration and so on. The mathematical model of the behavior of impurity ion in charge state z consists of the momentum conservation equation and the equation of continuity. The equation are written as follows,

for x impurity ion (Neuhauser et al.)

$$\rho_x\left(\frac{\partial}{\partial t} + \vec{V}_x\cdot\nabla\right)\vec{V}_x = -\nabla P_x + \vec{F}_x + \vec{R}_x + S_p^x - S_n^x \vec{V}_x \ ,$$

$$\vec{F}_x = q_x\vec{E} + q_x(\vec{V}_x \times \vec{B}) \ ,$$

$$\vec{E} = -\nabla P_e/en_e \ ,$$

$$\vec{R} = -\rho_x(\vec{V} - \vec{V}_x)/\tau_x - \frac{\rho_x}{m_x}\left[\alpha_x\nabla(kT_e) + \beta_x\nabla(kT_i)\right] \ ,$$

$$\alpha_x = 0.71\ Z^2 \ ,$$

$$\beta_x = -3\cdot\frac{1-\mu-5\sqrt{2}\ z^2\cdot(1.1\mu^{2.5} - 0.35\mu^{1.5})}{2.6 - 2\mu + 5.4\mu^2} \ ,$$

$$\mu = m_x/(m+m_x) \ ,$$

where S_p, S_n, $S_E^{i,e}$, $E_s^{i,e}$ and τ_x denote following meanings,

S_n : source term in mass conservation equation

S_p : momentum source term

$S_E^{i,e}$: energy source $\pm$ { $Q^{ei} - Q_{cx}$ / $Q^{ei} + Q_{rad}$

$E_s^{i,e}$: $E_s = \frac{3}{2}\frac{kT}{m} + \frac{1}{2}\vec{V}\cdot\vec{V}$

τ_x : Spitzer slowing down time

Temperature of impurity ion is assumed to be equal to that of fuel ion without solving the energy conservation equation.

The applicability of the code in relation to the combination of the ion species is summarized in Fig. 2. The code can treat four cases ((a) ∿ (d)) shown in the figure.

In Fig. 3, calculational mesh for FER reactor is shown. In the figure, the segments $\overline{AB}$, $\overline{BC}$, $\overline{CD}$, $\overline{DE}$, $\overline{EF}$ and $\overline{FG}$ correspond to the divertor plate and the sheath criterion is assumed at the place.

Calculational conditions used are as follows,

$$Q_T = Q_e + Q_i = 60 \text{ MW} ,$$

$$\Gamma_p = 1\times10^{22}s^{-1} , \quad 3\times10^{22}s^{-1} ,$$

$$\Gamma_{He^{2+}} = \Gamma_p \times 0.05 ,$$

respectively.

In Fig. 4, T_e profiles for particle fluxes of $1\times10^{22}s^{-1}$ and $3\times10^{22}s^{-1}$ are shown. The maximum temperature in the scrapeoff layer is approximately 210 eV at the j=8 flux tube. The e-folding length of T_e is nearly 3 cm. T_e decreases to approximately 20 eV at the divertor plate.

Density profile is shown in Fig. 5. Near the plate, $n_e \simeq 2\times10^{14}cm^{-3}$ for $\Gamma_p = 1\times10^{22}s^{-1}$ and $n_e \simeq 6\times10^{14}cm^{-3}$ for $\Gamma_p = 3\times10^{22}s^{-1}$ respectively. So we can see very high density build up near the divertor plate. The density around the boundary of the core plasma is roughly $7\times10^{12}cm^{-3}$ for $\Gamma_p = 1\times10^{22}s^{-1}$ and $1\times10^{13}cm^{-3}$ for $\Gamma_p = 3\times10^{22}s^{-1}$.

In Fig. 6, flow velocity of the fuel ion in the poloidal plane is shown. The flow in the j=9 flux tube which locates nearest to the boundary of the core plasma in the inboard side scrapeoff layer directs to the upper stream.

In Fig. 7, flow velocity in the poloidal plane for He^{1+} is shown. He^{1+} of the j=9 flux tube in the inboard side scrapeoff layer also go upstream. The spatial distribution of He^{1+} is comparatively uniform in the poloidal direction (i.e. not localized at the divertor region) such as fuel ions.

In Fig. 8 and Fig. 9, time evolution of the total mass and energy contained in the system is shown. From this figure we can see that after the 1200 step, mass and energy in the system do not change so distinctly. These results indicate the steady state is achieved after the step.

In Fig. 10, we show the energy flow into the divertor plate. The peak value at the outside and inside divertor plate is 310 $W\cdot cm^{-2}$ and 220 $W\cdot cm^{-2}$ respectively. As departing from the flux tube j=9 which locates nearest to the separatrix to j=5 flux tube, Q_e^d and Q_i^d decreases

rapidly and monotonically in the outside divertor. On the other hand, the second and third peaks appears in the inside divertor because of complicated shapes of the plate. In the estimation of the deposited energy flux, it is to be noticed that ionization energy loss should be counted in the sum. In this case of $\Gamma_p = 1\times10^{22}s^{-1}$ and $Q_T = 60$ MW, the ionozation energy loss is approximately 0.9 MW in the unit toroidal length.

Particle flux to the divertor plate Γ^d is shown in Fig. 11. The positions of the peak values also exist at the j=9 flux tube.

4. Summary

With a two-dimensional time dependent fluid code for the edge plasma in a Tokamak, preliminary numerical study has been carried out.

In the parameter of particle and energy flux from the core plasma to the scrapeoff layer Γ_p and Q_T of $\Gamma_p = 1\times10^{22}s^{-1}$ and $Q_T = 60$ MW, the maximum energy flux to the divertor plate Q_T^d is approximately 300 W/cm^2 and $4\times10^{19}s^{-1}cm^{-2}$ for particle flux. Furthermore, ionization loss energy in the unit toroidal length is about 1 MW/m.

Acknowledgements

It is a pleasure to acknowledge the support of Drs. S. Tamura, M. Yoshikawa, K. Tomabechi (JAERI), N. Asami (Mitsubishi Heavy Industries, Ltd.), T. Miura (Century Research Center Corporation) and M. Nishikawa (Mitsubishi Atomic Power Industries, Inc.).

rapidly and monotonically in the outside divertor. On the other hand, the second and third peaks appears in the inside divertor because of complicated shapes of the plate. In the estimation of the deposited energy flux, it is to be noticed that ionization energy loss should be counted in the sum. In this case of $\Gamma_p = 1\times10^{22}s^{-1}$ and $Q_T = 60$ MW, the ionozation energy loss is approximately 0.9 MW in the unit toroidal length.

Particle flux to the divertor plate Γ^d is shown in Fig. 11. The positions of the peak values also exist at the j=9 flux tube.

4. Summary

With a two-dimensional time dependent fluid code for the edge plasma in a Tokamak, preliminary numerical study has been carried out.

In the parameter of particle and energy flux from the core plasma to the scrapeoff layer Γ_p and Q_T of $\Gamma_p = 1\times10^{22}s^{-1}$ and $Q_T = 60$ MW, the maximum energy flux to the divertor plate Q_T^d is approximately 300 W/cm^2 and $4\times10^{19}s^{-1}cm^{-2}$ for particle flux. Furthermore, ionization loss energy in the unit toroidal length is about 1 MW/m.

Acknowledgements

It is a pleasure to acknowledge the support of Drs. S. Tamura, M. Yoshikawa, K. Tomabechi (JAERI), N. Asami (Mitsubishi Heavy Industries, Ltd.), T. Miura (Century Research Center Corporation) and M. Nishikawa (Mitsubishi Atomic Power Industries, Inc.).

rapidly and monotonically in the outside divertor. On the other hand, the second and third peaks appears in the inside divertor because of complicated shapes of the plate. In the estimation of the deposited energy flux, it is to be noticed that ionization energy loss should be counted in the sum. In this case of $\Gamma_p = 1\times10^{22}s^{-1}$ and Q_T = 60 MW, the ionozation energy loss is approximately 0.9 MW in the unit toroidal length.

Particle flux to the divertor plate Γ^d is shown in Fig. 11. The positions of the peak values also exist at the j=9 flux tube.

4. Summary

With a two-dimensional time dependent fluid code for the edge plasma in a Tokamak, preliminary numerical study has been carried out.

In the parameter of particle and energy flux from the core plasma to the scrapeoff layer Γ_p and Q_T of $\Gamma_p = 1\times10^{22}s^{-1}$ and Q_T = 60 MW, the maximum energy flux to the divertor plate Q_T^d is approximately 300 W/cm^2 and $4\times10^{19}s^{-1}cm^{-2}$ for particle flux. Furthermore, ionization loss energy in the unit toroidal length is about 1 MW/m.

Acknowledgements

It is a pleasure to acknowledge the support of Drs. S. Tamura, M. Yoshikawa, K. Tomabechi (JAERI), N. Asami (Mitsubishi Heavy Industries, Ltd.), T. Miura (Century Research Center Corporation) and M. Nishikawa (Mitsubishi Atomic Power Industries, Inc.).

References

[1] D.E. POST, C.E. SINGER, J. Nucl. Mater. 128 & 129 (1984) 78-90.

[2] M. PETRAVIC, D. POST, D. HEIFETZ, J. SCHMIDT, Phys. Rev. Lett. 48 (1982) 326.

[3] B.J. BRAAMS, P.J. HARBOUR, M.F.A. HARRISON, E.S. HOTSTON, J.B. MORGAN, J. Nucl. Mater. 121 (1984) 75-81.

[4] HARLOW, F.H., WELCH, J.E. (1965), 'Numerical calculation of time-dependent viscous incompressible flow', Phys. Fluids, 8, 2182.

[5] JAERI-memo 62-245

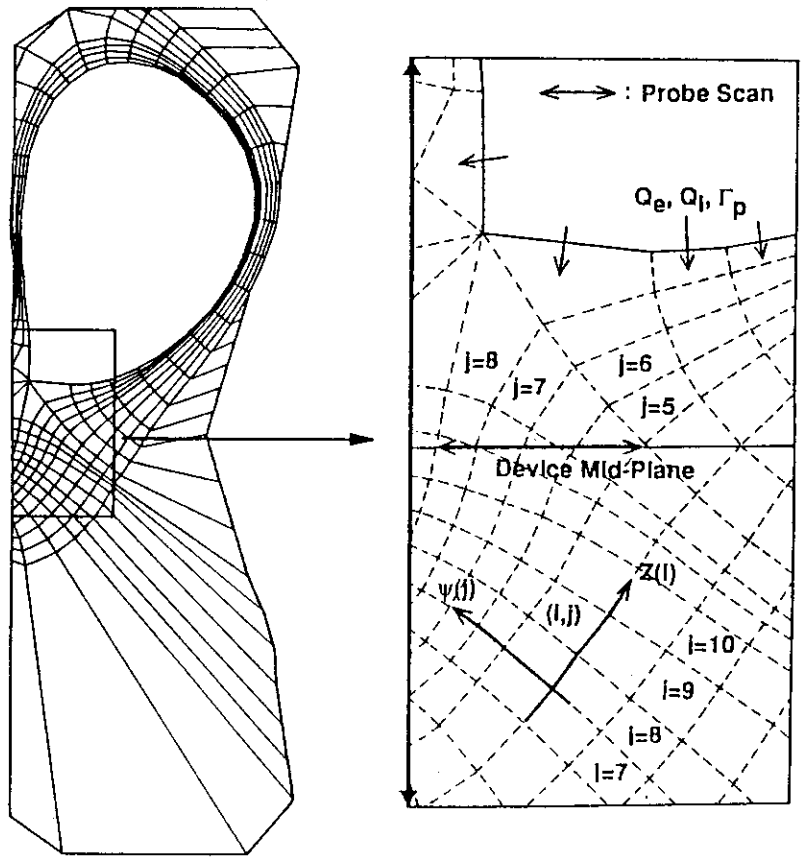

Fig. 1 The geometry, mesh and definition of the (z-ψ) coordinate system.

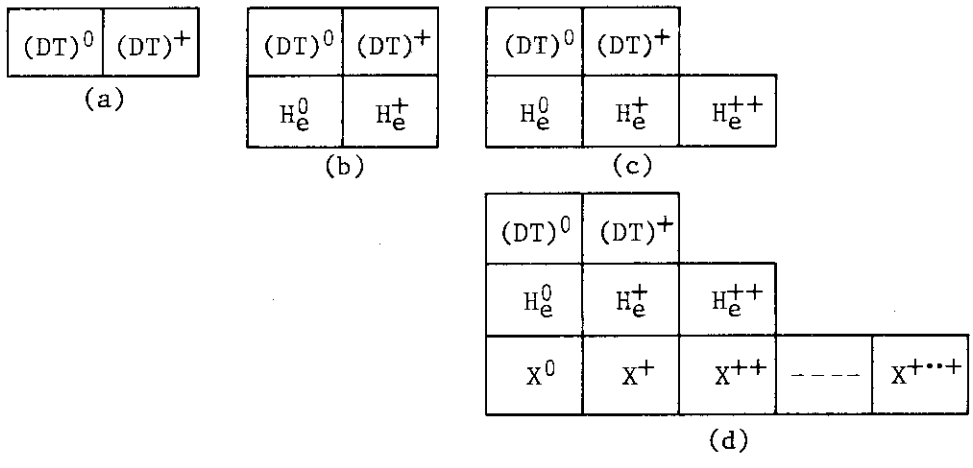

Fig. 2 Combination of the particle species included in the code. X denotes the impurity ion.

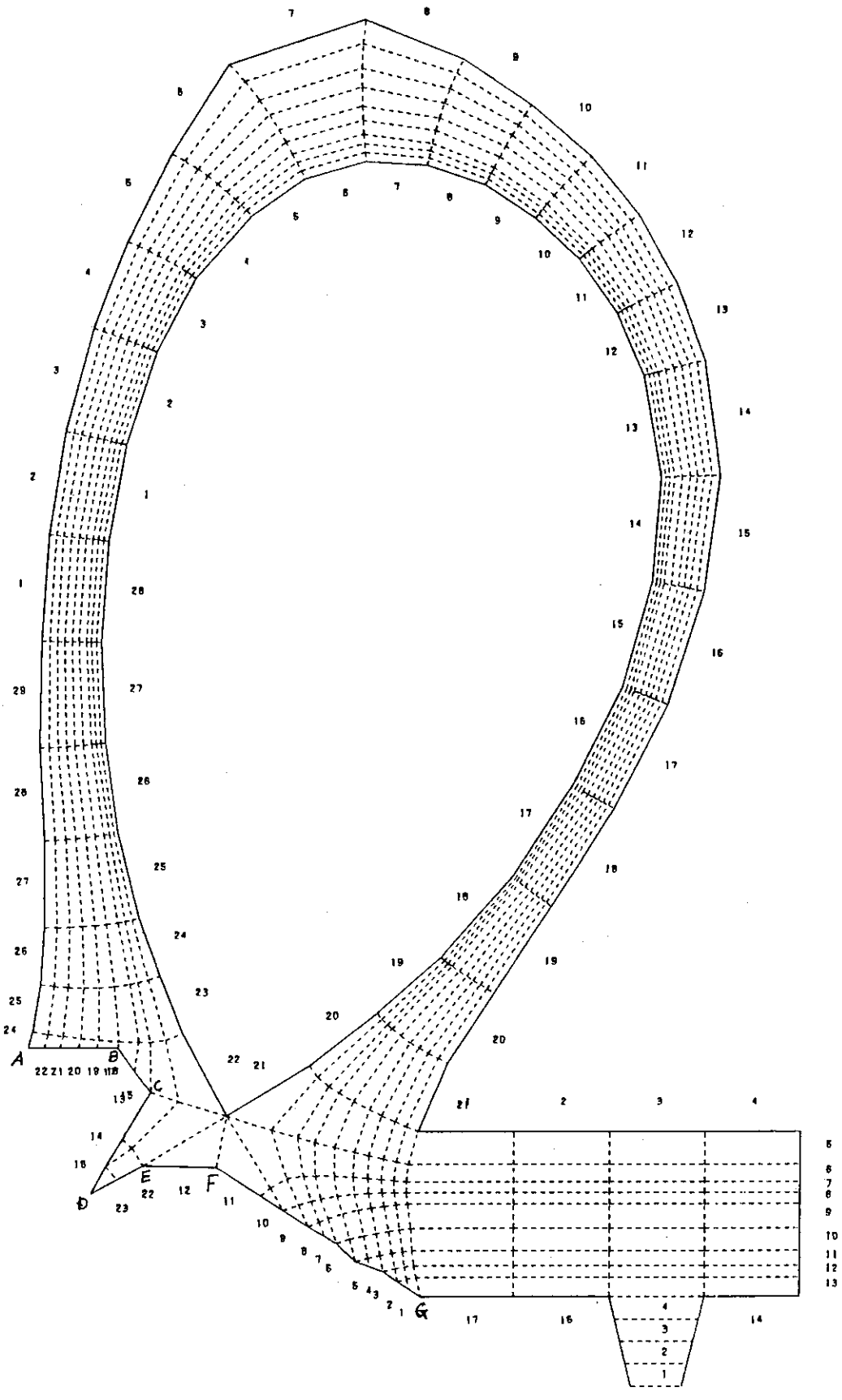

Fig. 3 Mesh used in the FER divertor analysis.

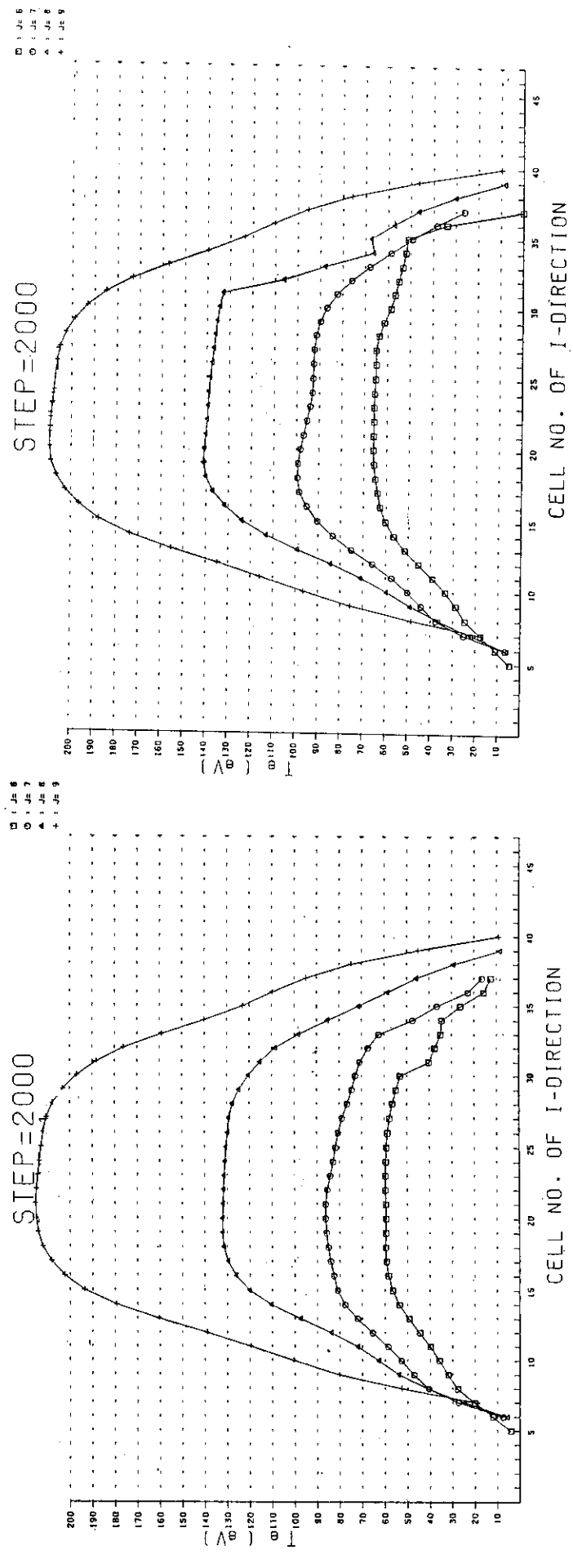

Fig. 4 T_e profiles in the poloidal direction for particle flux Γ_p of $1\times10^{22}s^{-1}$ and $3\times10^{22}s^{-1}$.

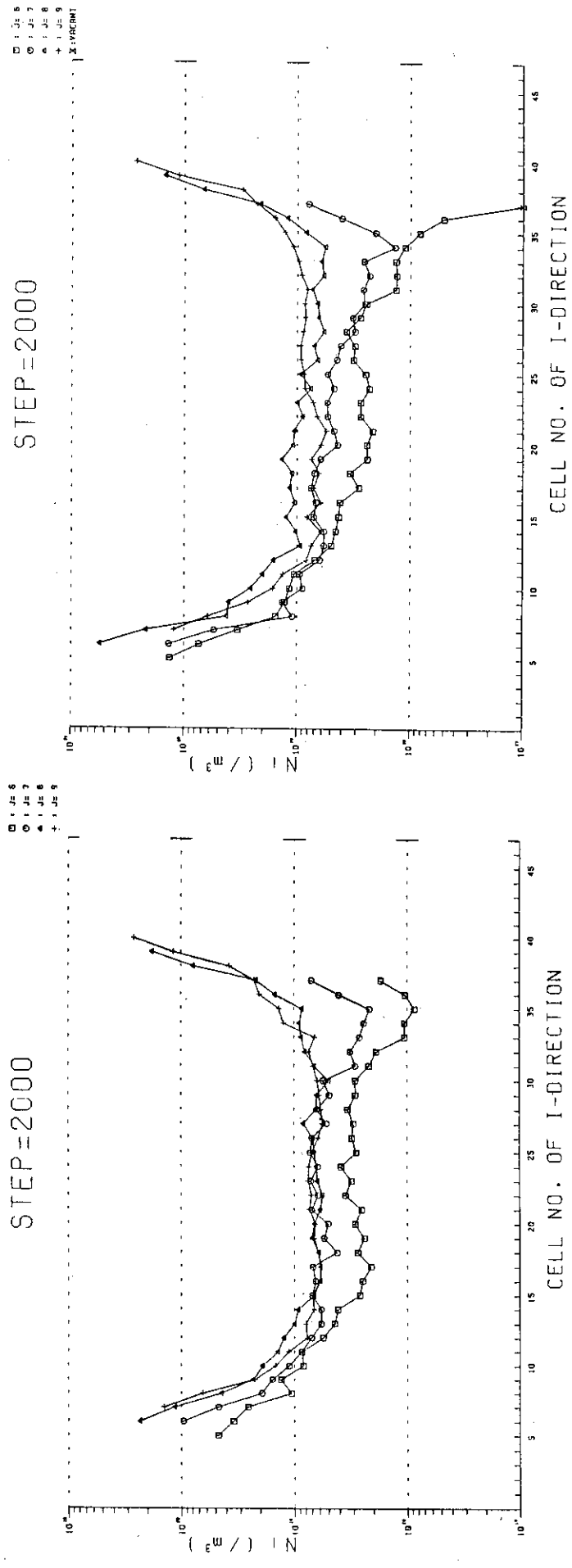

Fig. 5 Density profiles in the poloidal direction for particle flux Γ_p of $1\times10^{22}s^{-1}$ and $3\times10^{22}s^{-1}$.

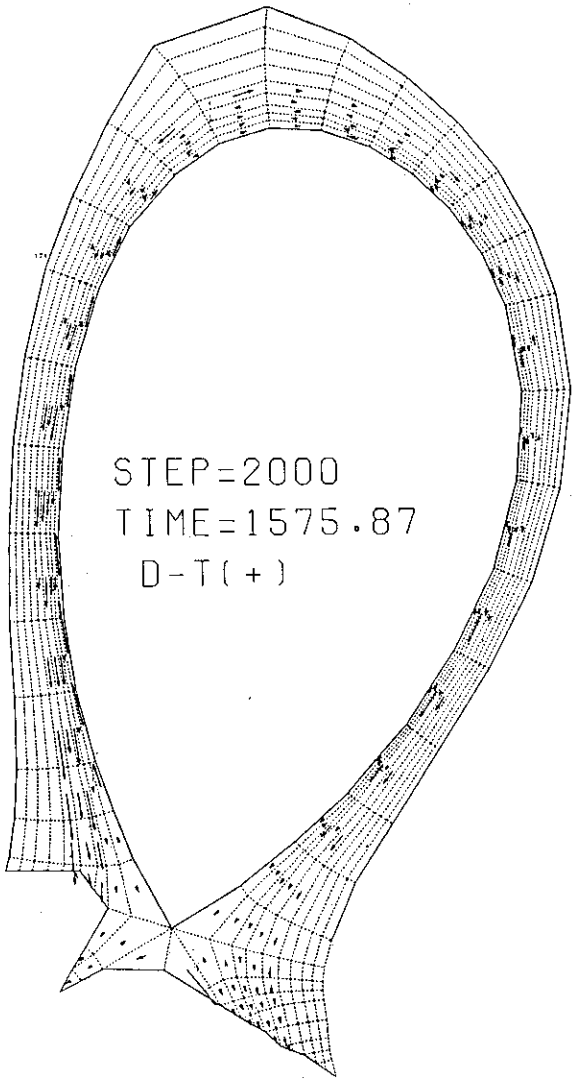

Fig. 6-a Flow velocity of the fuel ion for $\Gamma_p = 1\times10^{22}s^{-1}$.

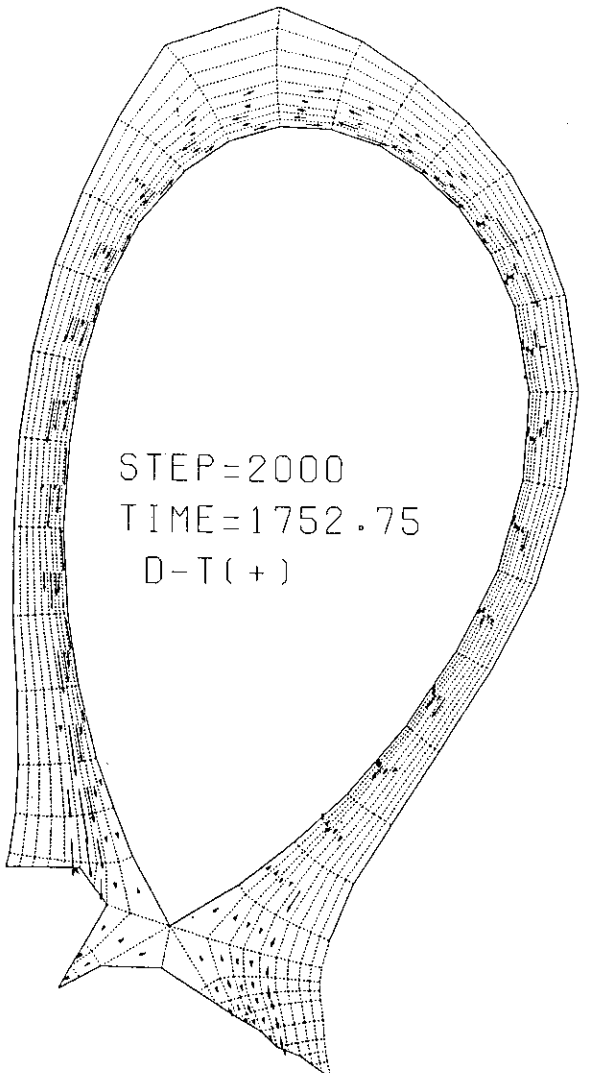

Fig. 6-b Flow velocity of the fuel ion for $\Gamma_p = 3\times10^{22}s^{-1}$.

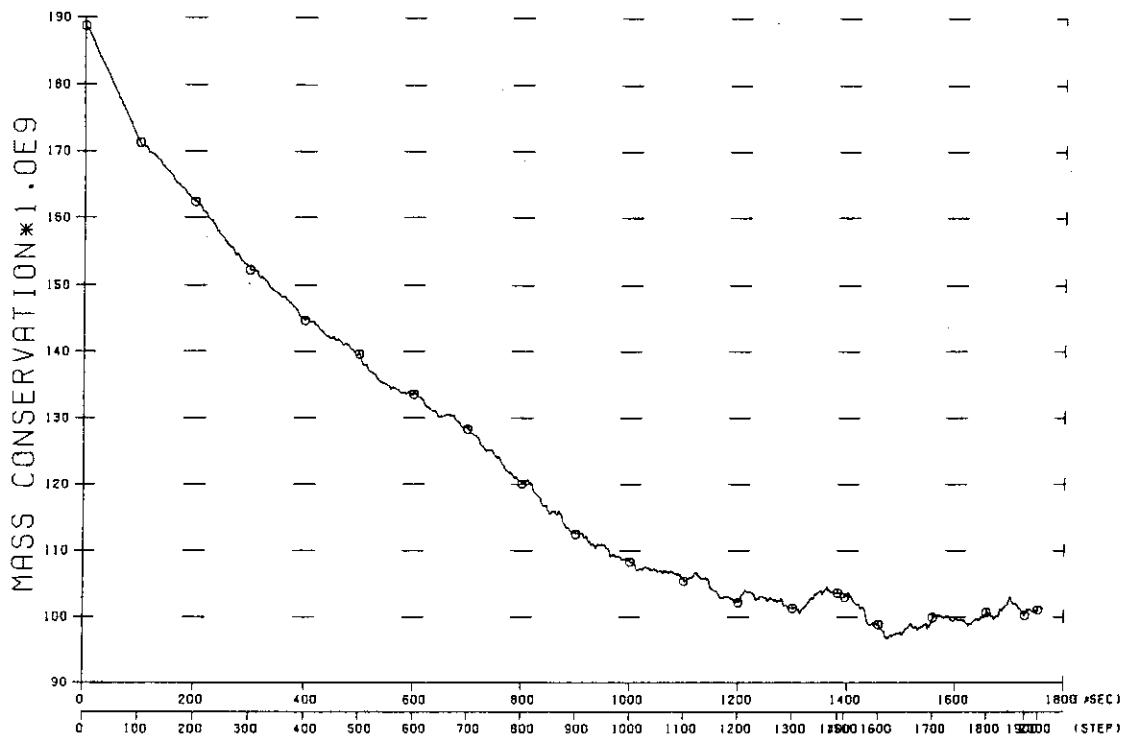

Fig. 8 Time evolution of the total mass in the system.

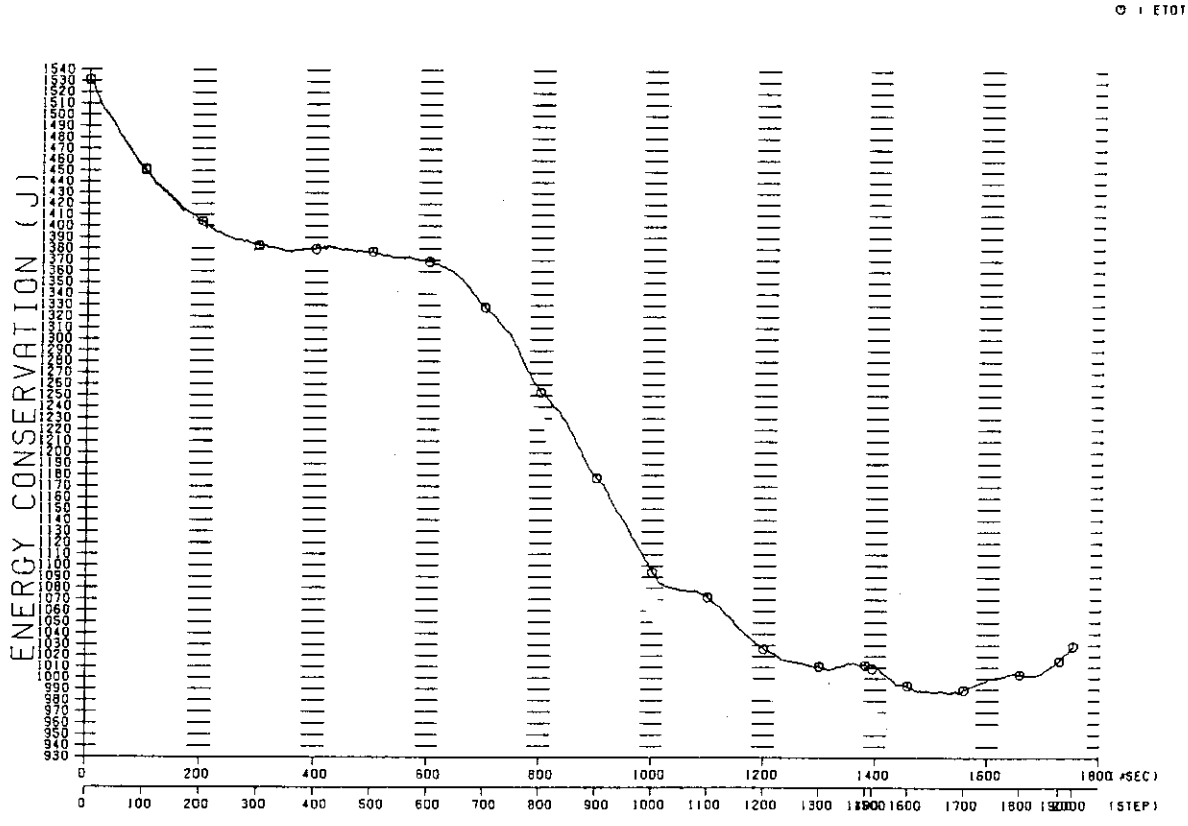

Fig. 9 Time evolution of the total energy in the system.

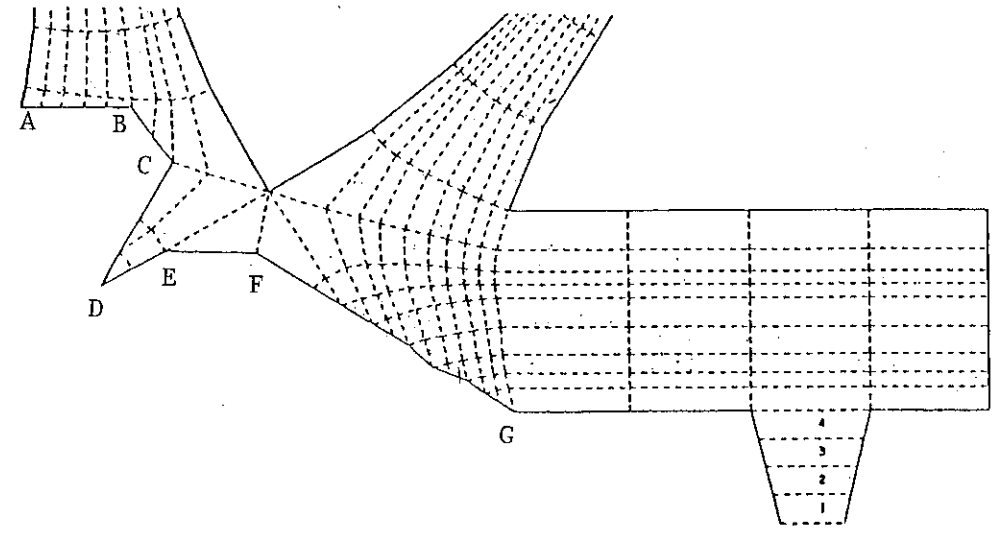

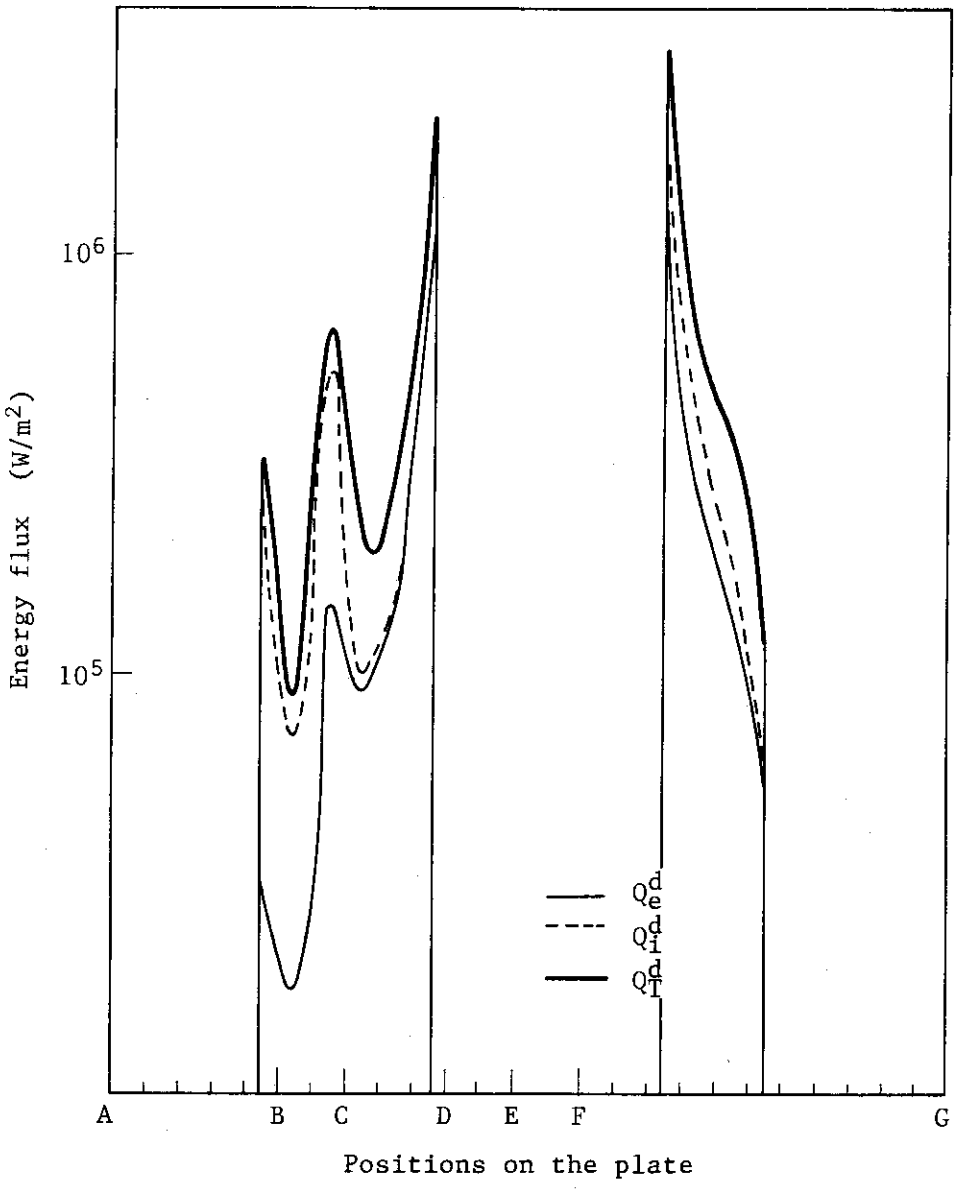

Fig. 10 Distribution of deposited energy flux Q^d on the divertor plate ($\Gamma_p = 1\times10^{22}$ s^{-1}).

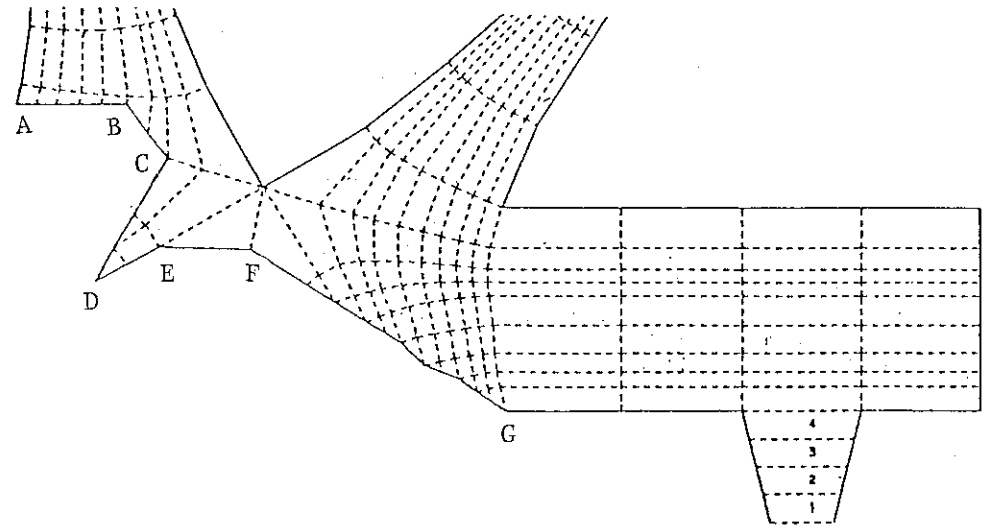

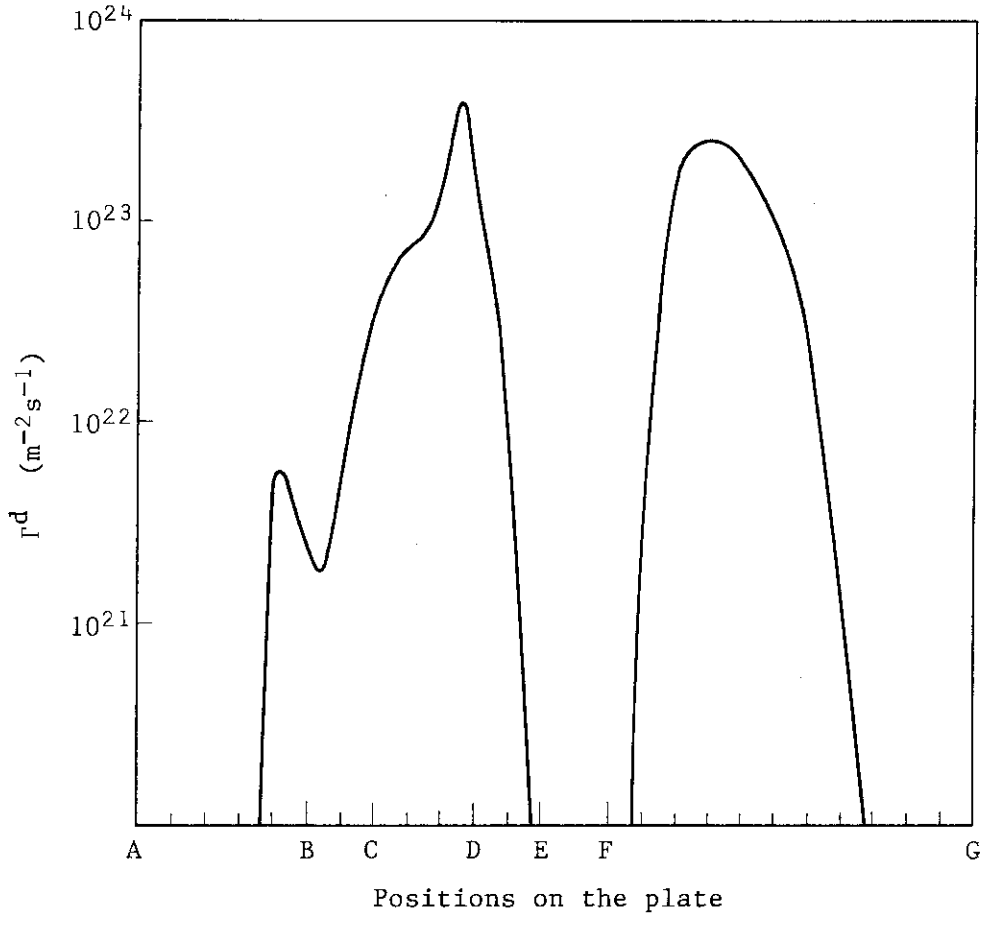

Fig. 11 Distribution of deposited particle flux Γ^d on the divertor plate ($\Gamma_p = 1\times10^{22}$ s^{-1}).